Auger recombination rates in nitrides from first principles

Kris T. Delaney

Materials Research Laboratory, University of California, Santa Barbara, CA 93106-5121

Patrick Rinke and Chris G. Van de Walle

Materials Department, University of California, Santa Barbara, CA 93106-5050

(Dated: October 29, 2018)

We report Auger recombination rates for wurtzite InGaN calculated from first principles density-functional and many-body-perturbation theory. Two different mechanisms are examined – inter- and intra-band recombination – that affect different parts of the emission spectrum. In the blue to green spectral region and at room temperature the Auger coefficient can be as large as $2\times10^{-30}\mathrm{cm^6s^{-1}}$; in the infrared even larger. Since Auger recombination scales with the cubic power of the free-carrier concentration it becomes an important non-radiative loss mechanism at high current densities. Our results indicate that Auger recombination may be responsible for the loss of quantum efficiency that affects InGaN-based light emitters.

Indium gallium nitride (InGaN) alloys are now already being used for light emitting and laser diodes in the green to ultraviolet part of the spectrum,[1] but increases in internal quantum efficiency (IQE) are still required to allow broader applications. The IQE of InGaN devices is limited by loss mechanisms that, at high drive currents (i.e., high carrier concentrations) lead to a decrease in IQE, a phenomenon commonly referred to as "efficiency droop". The precise nature of these loss mechanisms has been the subject of intense debate, and a variety of candidates have been proposed (see Ref. 2). Recently, Shen *et al.* suggested Auger recombination as the dominant source.[2,3] Loss due to Auger recombination scales with the cubic power of the free-carrier density and would thus dominate at the high carrier concentrations at which the reduction in IQE is observed. While Shen *et al.* found a cubic dependence of the IQE on the free-carrier concentration in optically pumped InGaN LED devices,[2] it is difficult to discriminate between different radiation-less processes experimentally. In this Letter we demonstrate by means of rigorous first-principles calculations, in which the Auger process can explicitly be isolated, that Auger recombination is indeed an important loss mechanism in wurtzite InGaN.

In the direct Auger process, an electron recombines with a hole, but instead of emitting a photon the process results in the excitation of another carrier to a higher-energy state (see insets of Fig. 1). This can also be viewed as two electrons colliding in the vicinity of a hole, resulting in a radiationless *e-h* recombination event, the energy and momentum of which is absorbed by the second electron (*eeh* process). Alternatively, the *hhe* process involves two holes and one electron. A first-principles description of the Auger recombination rate therefore requires an accurate calculation of the band structure and the transition probabilities for all relevant *eeh* and *hhe* processes as inputs.
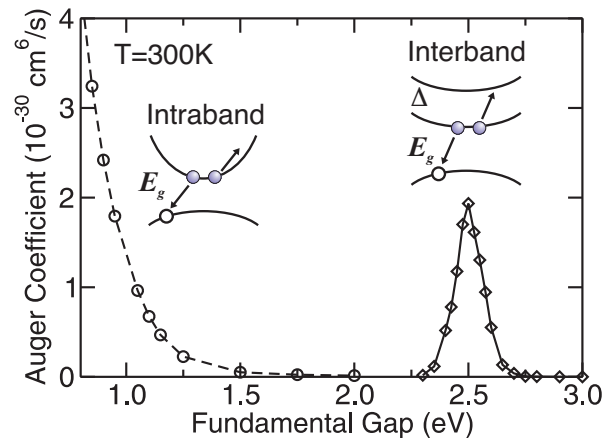
We obtain the band structures of the host ma-

FIG. 1: *eeh* Auger coefficient for light holes as a function of fundamental band gap for a simulated InGaN alloy (see text) at $T = 300\,\mathrm{K}$ and $n = 1\times10^{19}\,\mathrm{cm^{-3}}$. The statistical error bars of the Monte Carlo integration are smaller than the symbols for all data points presented. Intraband Auger, which involves scattering of an electron to an unoccupied part of the lowest conduction band (left inset, dashed line), dominates in In-rich alloys. However, for alloy concentrations relevant for solid-state lighting, interband Auger recombination, which involves scattering to the second-lowest conduction band (right inset, solid line), is dominant.

terials by combining density-functional theory (DFT) with many-body perturbation theory in the G_0W_0 approximation.[4] This approach accurately describes band structures of solids as measured by direct and inverse photoemission.[5,6,7,8] Combined with the exact-exchange optimized effective potential approach (OEPx(cLDA)) for the DFT part, it produces accurate band structures for AlN, GaN and InN in their zinc-blende and wurtzite phases.[9,10] We do not include spin-orbit coupling, which has only very small effects on the

band structure of nitrides. The results for wurtzite are shown in Fig. 2.

The Auger rate R is given by[11,12]

$$R = 2\frac{2\pi}{\hbar}\frac{V^3}{(2\pi)^9}\iiiint |M_{1,2,3,4}|^2 P_{1,2,3,4}$$
$$\delta(\mathbf{k}_{\text{sum}})\delta(E_{\text{sum}})\,d\mathbf{k}_1 d\mathbf{k}_2 d\mathbf{k}_3 d\mathbf{k}_4 \quad (1)$$

where states 3 and 4 are, e.g. for eeh, electrons in the conduction band and states 1 and 2 are a hole in the valence band and an electron in a higher-energy conduction-band state. $\mathbf{k}_{\text{sum}}$ and E_{sum} are short for $\mathbf{k}_1 + \mathbf{k}_2 - \mathbf{k}_3 - \mathbf{k}_4$ and $E_1 + E_2 - E_3 - E_4$, respectively. The statistics factor

$$P_{1,2,3,4} = (1 - f(E_1))(1 - f(E_2))f(E_3)f(E_4) \quad (2)$$

is determined by the Fermi occupation functions f, and $M_{1,2,3,4}$ are the Auger matrix elements of the screened Coulomb potential W

$$M_{1,2,3,4} = \langle\phi_1\phi_2|W|\phi_3\phi_4\rangle + \text{EX}, \quad (3)$$

where EX denotes exchange terms, as detailed in Ref. 13.

We compute $M_{1,2,3,4}$ directly with the OEPx(cLDA) wave functions and the non-local, dynamically screened Coulomb interaction W_0 from an RPA calculation. Our OEPx(cLDA) calculations were performed with the S/PHI/nX plane-wave pseudopotential code,[14] while for the G_0W_0 calculations we have employed the gwst space-time code.[15,16,17] With all operators being treated in real space, we have adapted the gwst code to compute the matrix elements of the screened Coulomb interaction in Eq. 3. In contrast with earlier work for semiconductors, the Auger matrix elements have been determined entirely from first principles. The calculations were performed at the experimental lattice constants reported in Ref. 10. For additional technical details and convergence parameters we refer to Refs. 7 and 9. We also note that a plane-wave cutoff of 17 Ha is required for the matrix elements such that the Auger rate is converged to within 10%.

For both eeh and hhe Auger processes we distinguish between *intra-* and *inter*-band events, depending on whether the final state of the scattered carrier lies in the same band as the initial state (see insets of Fig. 1). For typical concentrations of injected carriers (10^{17}–10^{20} cm^{-3}) holes and electrons are confined to a small region of the Brillouin zone around the Γ point. Assuming equal electron and hole concentrations the maximum momentum transfer to the Auger electron or hole that is scattered into the final state is $3k_F$ (at $T = 0$ K, where k_F is the Fermi momentum). Since energy and momentum have to be conserved in the Auger process, intraband Auger events are therefore only likely to occur for alloy compositions with small band gaps, as we demonstrate later. For larger band gaps intraband processes are negligible, and the possibility of interband Auger processes then depends on whether other valence or conduction bands are available into which holes or electrons can be scattered while energy is conserved. Our accurate band structures allow us to determine that possibility.

Focusing first on eeh processes, we note that the lowest conduction band in all three binary wurtzite phases is nondegenerate and almost spherically symmetric around the Γ-point. The next higher conduction band is situated at an energy Δ above the CBM at Γ ranging from 2.5 to 3.1 eV (see Fig. 2 and Table I). This strongly suggests that interband eeh Auger processes that excite an electron into this second conduction may occur for InGaN alloys with matching band gaps. This second conduction band was not included in a recent $k.p$ study by Hader *et al.*, leading them to conclude that direct Auger losses are negligible in InGaN quantum wells.[18]

The formidable computational challenges involved in calculating Auger rates were discussed by Laks *et al.*[11] The calculation of the Auger recombination rate itself [Eq. (1)] scales with the fourth power of the number of k points, rendering explicit integration over a grid of k points prohibitively expensive. We therefore tackled this multidimensional integration with a Monte Carlo approach. We compute statistical averages over 40,000,000 Monte Carlo steps, chosen so that the error of the mean is always at least one order of magnitude lower than the value of the mean. Because of the expense involved in a first-principles calculation of Auger matrix elements [Eq. (3)], we confined the calculations to a finite number of points in the twelve-dimensional k-space (10,000 elements in total), and employed a linear-interpolation scheme for k points off the mesh. This approach is justified because we found that the matrix elements vary only weakly over the small volume of the Brillouin zone involved in Auger recombination. Accurate interpolations of the OEPx(cLDA)+G_0W_0 band structures were obtained using an anisotropic effective-mass model.[10]

Our present calculations are aimed at examining Auger rates for a wide range of InGaN band gaps. Explicit evaluation of band structures and wave functions for each of the corresponding alloy compositions would be prohibitive. We performed calculations entirely from first-principles for eeh processes in pure GaN, and modeled different alloy compositions by applying a "scissor shift" to the band gap (i.e., rigidly shifting all conduction bands relative to the valence bands). While this choice is not optimal for calculations of alloys with large In concentrations, we note that In concentrations in current optoelectronic devices do not exceed 15% and thus an extrapolation of band parameters and matrix elements from GaN is the most sensible choice. With each E_g value we associate an alloy composition by using a bowing parameter $b = 2.5$ eV,[19] and then use linear interpolation to obtain Δ based on the values listed in Table I. This approach is justified by the similarity of the wave functions and band structure for corresponding bands of GaN and InN.

The Auger coefficient, defined as $C = R/n^3$, is reported in Fig. 1 as a function of the fundamental band gap for $T = 300$ K and a carrier density of 1×10^{19} cm^{-3}. For the purposes of the figure, we populated only the light-hole band with holes. Holes in other valence bands lead to a similar magnitude of the Auger coefficient. In
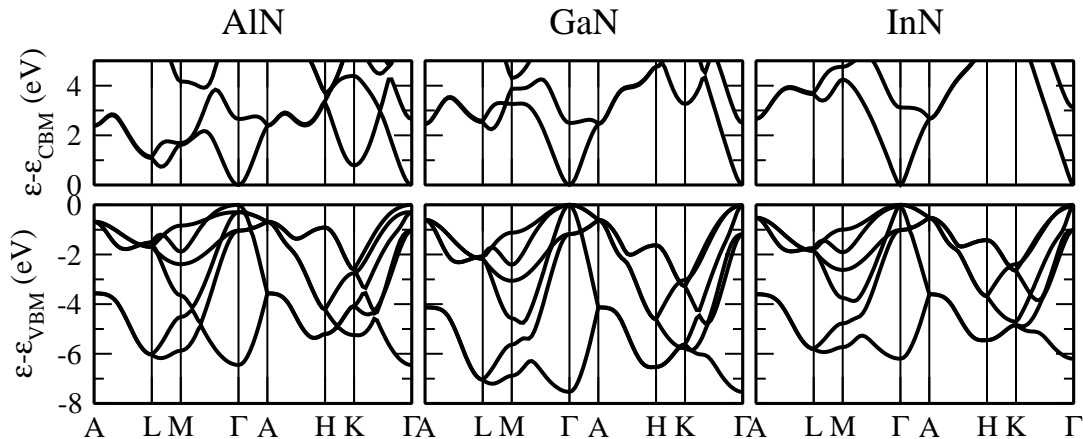
FIG. 2: OEPx(cLDA)+G_0W_0 band structure for wurtzite AlN, GaN and InN. For ease of comparison the valence bands have been aligned at the valence-band maximum (VBM) and the conduction bands at the conduction-band minimum (CBM).

	wurtzite			zinc blende		
	AlN	GaN	InN	AlN	GaN	InN
E_g	6.47	3.24	0.69	6.53	3.07	0.53
Δ	2.65	2.50	3.12	8.62	9.07	10.12
Δ_c	−0.295	0.034	0.066			

TABLE I: Band gap (E_g), gap between the first and the second conduction band at Γ (Δ) and crystal-field splitting (Δ_c) calculated with the OEPx(cLDA)+G_0W_0 approach for AlN, GaN and InN.

our calculations, which use Fermi-Dirac statistics, the Auger coefficient is largely independent of n for densities up to $1 \times 10^{19}\,\mathrm{cm}^{-3}$. We note that the interband process has a weak dependence on the choice of bowing parameter due to the method of choosing Δ. For b ranging from 1 to 4 eV, the center of the recombination peak varies by less than 0.1 eV.

Three distinctly different regimes emerge. For large band gaps, intraband Auger recombination is negligible and interband recombination dominates. For small band gaps (< 1.0 eV) the situation is reversed. In an intermediate energy region, both eeh recombination processes are irrelevant. The two Auger regimes exhibit a different characteristic behavior as a function of band gap: while interband recombination peaks when Δ and E_g are in resonance, intraband recombination monotonically increases with decreasing band gap. hhe processes are not included here, but inspection of the band structures in Fig. 2 allows us to conclude that they do not contribute at E_g values above 2.5 eV.

The Auger coefficients computed with our model fall within the (very wide) experimentally reported range of 1×10^{-34} to $5 \times 10^{-28}\,\mathrm{cm}^6\mathrm{s}^{-1}$ (Ref. 2). In particular, they agree well with the values reported by Shen *et al.*[2] based on their optical pumping experiments. Their reported Auger coefficient ranged from $(1.4 - 2.0) \times 10^{-30}\,\mathrm{cm}^6\mathrm{s}^{-1}$

and increased with In concentrations rising from 9 to 15%. Our calculated values in Fig. 1 are in qualitative and quantitative agreement with these observations, strengthening the case that the observed losses are indeed due to Auger recombination. Interestingly, Fig. 1 shows that the Auger coefficient continues to increase when the band gap is lowered down to 2.5 eV; i.e., for longer wavelengths. This indicates that rising Auger losses could well play an important role in the "green gap" problem, the well known decrease in efficiency of InGaN light emitters at longer emission wavelengths.

Based on our results we can examine possible strategies for reducing Auger losses in the blue/green region of the spectrum. (1) Using the zinc-blende phase, in which the second conduction band occurs at much higher energies (see Table I); however, growth of high quality phase-pure zinc-blende nitrides has proven very difficult. (2) Strain engineering the band structure to move the second conduction band away from the resonance; however, both the first and second conduction band are nondegenerate and thus sensitive only to hydrostatic strain, and our calculated deformation potential for the energy difference Δ is quite small. (3) Tuning InGaAlN alloy compositions. Again, this is likely to be fruitless because the value of Δ is similar for all three nitrides (Table I).

In summary, we have presented first-principles evaluations of Auger recombination rates in InGaN alloys, showing the presence of a resonance that leads to increasing values of the Auger coefficient for wavelengths ranging from blue to green. The calculated values are in good agreement with experiment and confirm that Auger recombination is a key loss mechanism in nitride light emitters.

[1] S. Nakamura and S. F. Chichibu, eds., *Introduction to Nitride Semiconductor Blue Lasers and Light Emitting Diodes* (Taylor and Francis, London, 2000).

[2] Y. C. Shen, G. O. Mueller, S. Watanabe, N. F. Gardner, A. Munkholm, and M. R. Kramers, Appl. Phys. Lett. **91**, 141101 (2007).

[3] N. F. Gardner, G. O. Müller, Y. C. Shen, G. Chen, S. Watanabe, W. Götz, and M. R. Kramers, Appl. Phys. Lett. **91**, 243506 (2007).

[4] L. Hedin, Phys. Rev. **139**, A796 (1965).

[5] W. G. Aulbur, L. Jönsson, and J. W. Wilkins, Solid State Phys. : Advances in Research and Applications **54**, 1 (2000).

[6] G. Onida, L. Reining and A. Rubio, Rev. Mod. Phys. **74**, 601 (2002).

[7] P. Rinke, A. Qteish, J. Neugebauer, C. Freysoldt, and M. Scheffler, New J. Phys. **7**, 126 (2005).

[8] P. Rinke, A. Qteish, J. Neugebauer, and M. Scheffler, phys. stat. sol. (b) **245**, 929 (2008).

[9] P. Rinke, A. Qteish, M. Winkelnkemper, D. Bimberg, J. Neugebauer, and M. Scheffler, Appl. Phys. Lett. **89**, 161919 (2006).

[10] P. Rinke, M. Winkelnkemper, A. Qteish, D. Bimberg, J. Neugebauer, and M. Scheffler, Phys. Rev. B **77**, 075202 (2008).

[11] D. B. Laks, G. F. Neumark, and S. T. Pantelides, Phys. Rev. B **42**, 5176 (1990).

[12] A. Haug, D. Kerkhoff, and W. Lochmann, Phys. Stat. Sol. B **89**, 357 (1978).

[13] B. K. Ridley, *Quantum Processes in Semiconductors*, (Clarendon, Oxford, 1982), p. 268.

[14] http://www.sphinxlib.de.

[15] M. M. Rieger, L. Steinbeck, I. White, H. Rojas, and R. Godby, Comput. Phys. Commun. **117**, 211 (1999).

[16] L. Steinbeck, A. Rubio, L. Reining, M. Torrent, I. White, and R. Godby, Comput. Phys. Commun. **125**, 105 (2000).

[17] C. Freysoldt, P. Eggert, P. Rinke, A. Schindlmayr, R. W. Godby, and M. Scheffler, Comput. Phys. Commun. **176**, 1 (2007).

[18] J. Hader, J. V. Moloney, B. Pasenow, S. W. Koch, M. Sabathil, N. Linder, and S. Lutgen, Appl. Phys. Lett. **92**, 261103 (2008).

[19] S. Stepanov, W. N. Wang, B. S. Yavich, V. Bougrov, Y. T. Rebane, and Y. G. Shreter, MRS Internet J. Nitride Semicond. Res. **6**, 6 (2001).